



Experimentally validated CFD analysis on sampling region determination of average indoor carbon dioxide concentration in occupied space

Anna Bulińska ^{a,*}, Zbigniew Popiółek ^a, Zbigniew Buliński ^b

^aDepartment of Heating, Ventilation and Dust Removal Technology, Silesian University of Technology, Konarskiego 20, 44-100 Gliwice, Poland

^bInstitute of Thermal Technology, Silesian University of Technology, Konarskiego 22, 44-100, Gliwice, Poland



ARTICLE INFO

Article history:

Received 15 August 2013

Received in revised form

29 October 2013

Accepted 2 November 2013

Keywords:

Metabolic carbon dioxide
Pollution spatial distribution
Representative sampling area
Computational fluid dynamic (CFD)

ABSTRACT

Measurements of carbon dioxide concentration become a very popular method for determination of the air exchange rate in buildings. In measurement practice applied by many researches only one sensor is used in a single room. This cause that the measured CO₂ concentration should represent mean concentration in the room. This cause that the positioning of the CO₂ sensors is crucial for such a measurements. This paper attempts to find representative measuring area of mean CO₂ concentration in a particular room with one sleeping person using numerical modelling. Different parameters that determine CO₂ distribution in the room were analysed. Results show that the geometry of the window opening and internal heat sources have a significant influence on a spatial distribution of CO₂. It was found that simplified exhalation compared to a full breathing model of the person is enough precise for accurate CO₂ distribution analyses. Representative area of CO₂ concentration spreads over the half of the room. CO₂ sensors can be positioned in the centre of the room or moved towards the door were the air flows out. Positions which should be avoided during the measurements were in the vicinity of the radiator and window. In case of the sleeping person all the space over the sleeping person must be excluded from the measurements. The distance of the sensor from the wall should be at least 40 cm. The measurements can be successfully made in the centre of the room independently of the room height.

© 2013 Elsevier Ltd. All rights reserved.

1. Introduction

Knowledge of the ventilation air change rate is crucial to control indoor air quality in occupied buildings. A very restrictive energy savings regulations for buildings caused limitation of the natural air leakage to buildings. Reduced ventilation in many naturally ventilated buildings in Europe caused increased concentration of indoor air pollution and very poor indoor air quality [1–4]. In poorly ventilated buildings occupants can suffer from many health problems which are particularly frequent among children [5]. This cause that the ventilation measurements are of great importance for the estimation of the indoor air exchange rate and for assessment of the indoor air quality. There is a number of the approaches used to evaluate building ventilation and indoor air quality [6,7]. One of the method widely used by researches nowadays are measurements of metabolically generated carbon dioxide concentration [3,8–13]. Such measurements are simple and quiet cheap comparing to other

tracer gas methods. The main advantage of this method is carrying out measurements in occupied spaces during they normal exploitation. Carbon dioxide measurements are very popular in naturally ventilated residential buildings, offices and classrooms.

The carbon dioxide is present in the atmospheric air with concentration at the typical value of 350 ppm [14]. In the buildings people are the main sources of the carbon dioxide. Exhaled air contains 4–5% of carbon dioxide. This amount depends on the activity level and the size of the occupants [15,16]. Increase of the carbon dioxide concentration in the room depends on the source strength and the amount of the fresh air entering the space that dilutes the carbon dioxide concentration. The CO₂ concentration levels that occur indoors are harmless and not perceived by humans, but they are a good indicator of other bioeffluents from people being perceived [17]. Many standards define acceptable level for the carbon dioxide concentration to keep comfort criteria of the indoor air quality. ASHRAE Standard 62 states that comfort criteria are satisfied if the ventilation rate is enough to keep carbon dioxide level under 1000 ppm [18]. This is the commonly referenced guideline value for carbon dioxide concentration in the literature [2–4,12,19,20].

* Corresponding author. Tel.: +48 322372830; fax: +48 322372559.

E-mail address: anna.bulinska@polsl.pl (A. Bulińska).

If the carbon dioxide concentration is higher than the outdoor level it can be used as a tracer gas to calculate air exchange rate [15,21–23]. Knowing the source emission and outdoor concentration air change rate can be calculated from the mass balance equation of the carbon dioxide

$$V \frac{dC}{dt} = Q \cdot C_0 - Q \cdot C + F \quad (1)$$

where: V is volume of the room, Q is the air flow through the room, C is internal concentration of CO_2 , C_0 is concentration of the CO_2 in the surrounding, F is CO_2 emission from people and t is time.

The main problem that occurs during the measurements of the carbon dioxide concentration is sampling point density and position of the sensor [11,24]. Calculation method of the air change rate assumes homogeneous concentration of the carbon dioxide in the whole space. Most researches prefer to use only one sensor in the room [11]. This cause that the measurement at one sampling point in the space is taken to represent average concentration in that space. For that reason the sampling location of the sensor must be selected very carefully.

In naturally ventilated rooms no additional air mixing is used. Air velocity observed in rooms with closed doors and windows are usually very small. In such a case carbon dioxide is distributed mainly by diffusion while advection is less important. This results in non-uniform carbon dioxide concentration field with the regions of the lower and higher concentration over the average in the whole room. Previous researches performed by Barankova [8], Naydenov [9] and Mahyuddin and Awbi [10] confirms non-uniform distribution of carbon dioxide in the rooms. Naydenov [9] noted deviations of carbon dioxide concentration from the average value of 50 ppm during occupants absence which increased up to 270 ppm during the night. Similar survey in the climatic chamber conducted Barankova [8] and Mahyuddin and Awbi [10]. Mahyuddin and Awbi have found that higher concentrations occurs in the higher parts of the room over 1.8 m.

Common guidelines for carbon dioxide sampling point positions can be found in standards for tracer gas measurements. The ASTM standard E 741-00 [25] devoted to tracer gas measurements in the single zone suggests that at the representative locations throughout the zone the gas concentration shell differ by less than 10% of the average concentration for the zone. ASTM Standard D 6245-07 states only that carbon dioxide concentrations can not be made too close to people. Representative locations should be predicted by the measurements at the multiple locations that yields a representative value. A large survey on representative sampling points for carbon dioxide concentration preferences is presented in [11]. That survey were based on the literature and questionnaire study of researches practice and found that the majority of the researches and respondents preferred heights between 1.0 m and 1.2 m.

Investigations of the carbon dioxide distribution within closed spaces published so far in the literature were based mainly on the in situ measurements. Due to non-perfect mixing of exhaled carbon dioxide in the room it is very difficult to analyse its spatial distribution in space. With a limited number of CO_2 sensors, measurements are only performed in the limited number of points in the space. On the other hand a numerical simulation provides carbon dioxide concentration in all points of the computation domain. There has been some researches that focussing on the numerical modelling of carbon dioxide spatial distribution in different occupied spaces [26–28].

The objective of this paper is to analyse the distribution of CO_2 exhaled by person in order to define sampling area of the average carbon dioxide concentration in the room for determination of air

change rate. This paper deals with a numerical modelling of spatial distribution of carbon dioxide in a room with one sleeping person. Along with numerical calculation, a set of measurements were carried out. Only the night hours were used for the numerical calculations. Results of the measurements previously made by the author showed that the best for the calculations of the air exchange rate are measurements at night hours with build up of carbon dioxide concentration or during the day when occupants are absent [29]. During these two periods carbon dioxide concentration are almost monotonic. In comparison during the day recorded concentration were influenced by many fluctuations that occurs under normal occupation related with doors and windows opening and closing as well as occupants movements. Measurement in a room with one sleeping person was used to validate the numerical model.

2. Experimental investigation of carbon dioxide and temperature distribution in the room

2.1. Experimental set up

Experimental investigation of the spatial distribution of the metabolic CO_2 was performed in a single room of apartment. The apartment was located on the fourth floor of the six storeys building (Fig. 1a). The building is naturally ventilated. Air enters

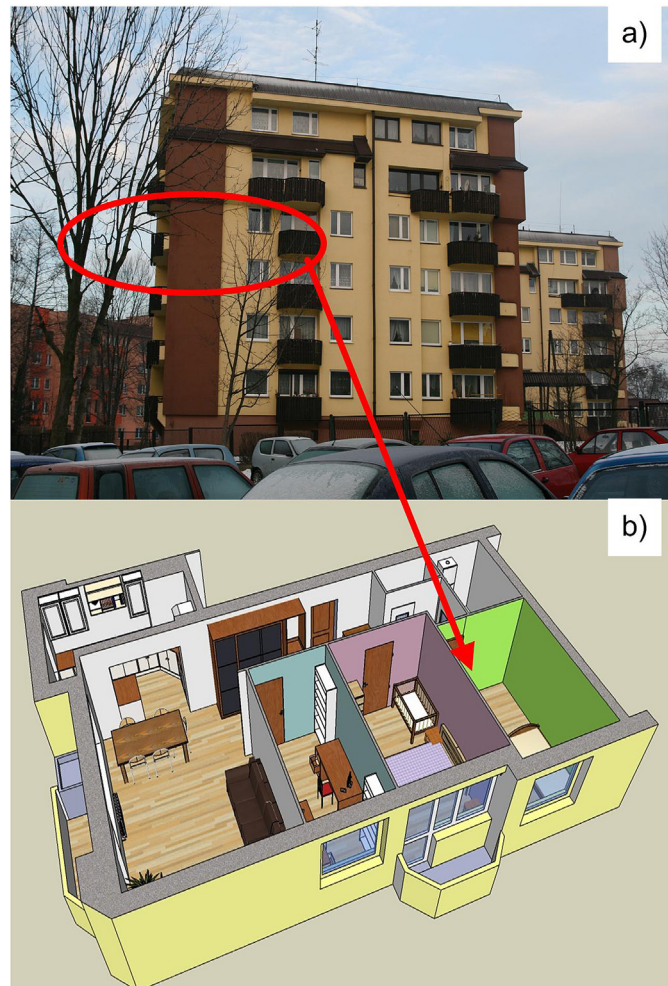


Fig. 1. The layout of the a) building and b) apartment in which the experiment was performed.

Table 1

Technical data of the IAQ sensors PS30.

Parameter	Measurement range	Sensitivity repeatability
Carbon dioxide, ppm	0 ÷ 5000	±(20 ppm + 3% measured value)
Humidity %	0 ÷ 100	±3.5
Temperature, °C	10 ÷ 45	±0.5
Barometric pressure, hPa	900 ÷ 1100	±3

building through the cracks in the building envelope (mainly doors and windows) and exit through the ventilation duct. The experiment was carried out at the beginning of May during the night hours. The experiment was repeated during three consecutive nights. The only source of carbon dioxide in the room during the experiment was one sleeping person. Spatial distribution of carbon dioxide was measured using Indoor Air Quality Sensors PS30 (IAQ Sensors). IAQ Sensors are equipped with carbon dioxide, temperature and humidity sensors, they also measure barometric pressure of air. The technical parameters of used sensors are presented in Table 1. Sensors recorded data with one minute intervals. CO₂ sensors were calibrated before the experiment. Four sensors were placed inside the room (monitor 1–20 cm under the ceiling, monitor 2 – in the room corner, monitor 3 – on the floor in the centre of the room, monitor 4 – next to bed 45 cm above the floor) and one outside the building (Fig. 2). The room orientation in the apartment is shown in Fig. 1b.

The other measured quantities during the experiment were temperature of the walls, velocity in the door gap and temperature of the sleeping person covered with duvet. Temperatures of the walls and window surfaces were measured with thermocouples. Nine thermocouples were placed on the walls, two were attached to window and one thermocouple was measuring an ambient temperature. Velocity and temperature of the air blowing out of the room were measured with the thermoanemometer in the door gap every half a minute during the measurements. Temperature of the human body surface was recorded with the infrared camera. Data from measurements was used to determine the initial and boundary conditions for the CFD simulation.

2.2. Measurements

Fig. 3 shows carbon dioxide concentration, temperature and velocity variation in time measured during the experiment. Before

the experiment started the room was ventilated. It resulted in the uniform indoor air conditions within the whole room at the beginning of experiment. After the airing period the window was closed and one person entered the room and went to sleep. This started the main part of the experiment which lasted at least about three hours every day. In Fig. 3 small difference of carbon dioxide concentration in different sampling locations were observed. Analysing data from the subsequent days it was found that the highest carbon dioxide concentration appears in the upper part of the room (measured by sensor 1) and lower close to the floor (measured by sensor 2 and 3). Results presented by Mahyuddin and Awbi [10] confirm vertical stratification of carbon dioxide in the room with higher concentrations in the higher parts of the room and lower close to the floor. Air temperature measured during the experiment was slowly increasing after closing the window reaching around 22 °C at the end of the experiment. Humidity in the room was about 40% at the beginning of the experiment and increased only a several percent during the night.

Small variations within the range of 2 °C of the wall temperature were observed. The lowest temperature was observed on the external wall and surface of the window. The velocity measured in the door gap was 0.8 m/s. Air exchange rate calculated from the velocity in door gap was equal 1 h⁻¹ with measurement uncertainty about 13%. Recorded data from the experiment was used in the numerical calculations as a boundary and initial conditions. Results of time history of carbon dioxide concentration was used to compare them with results of numerically calculated curves.

3. Outline of numerical model

3.1. Geometry

A three dimensional model of the room interior was build for the purpose of numerical calculations. The geometry was based on the dimensions of the real room from the experiment. Two geometries were considered for the calculations one simplified and one detailed as presented in Fig. 4. The first geometry has a simplified supply opening at the top of the window (Fig. 2a). The second one has an infiltration slit along the part of the window perimeter. Moreover in the second model more details of the room geometry were included e.g. window-board and radiator. In both case of the model the window opening has the same area of 0.0086 m².

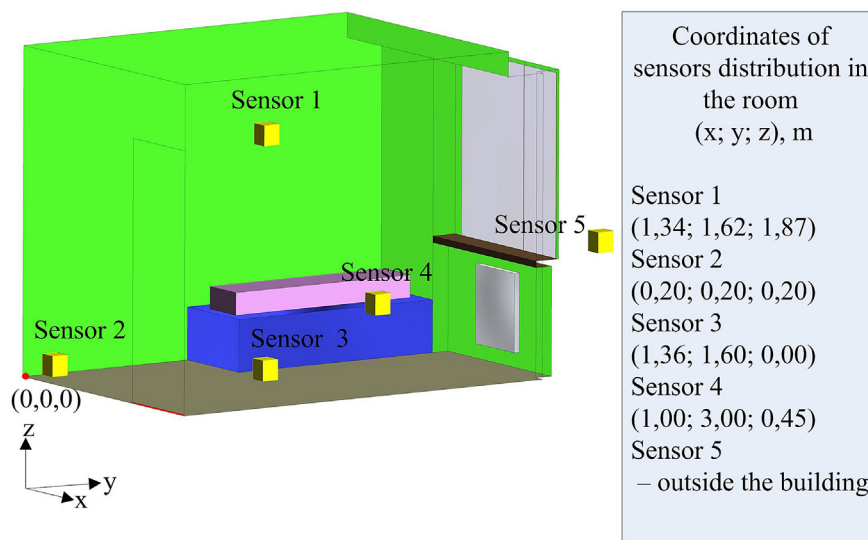


Fig. 2. Spatial distribution of IAQ sensors in the room.

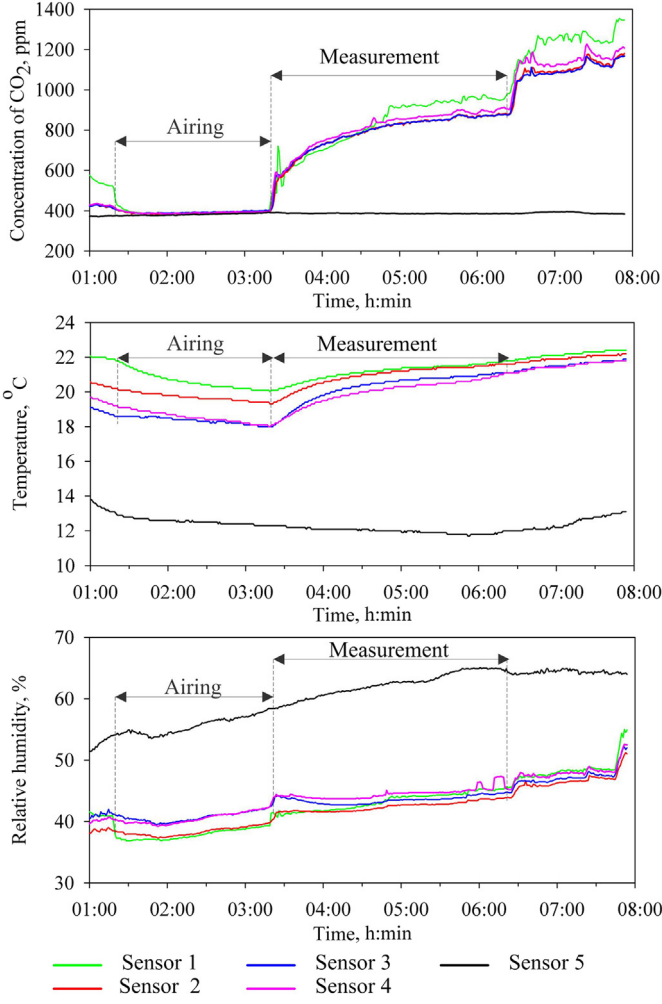


Fig. 3. Time history of the air parameters measured in the room by IAQ sensors.

The air was leaving the room through the crack in the door gap. The room was occupied by one person sleeping facing up on the bed. Geometry of the person was simplified to a cuboid shape ($180 \times 30 \times 17 \text{ cm}^3$). Benchmark tests preformed by Deevy [30]

shows that similar results of the modelling were found for simplified and precise geometry of the human. The main differences appeared only close to the person, which can have importance for thermal comfort modelling. Dimensions of the cuboid were base on the body area of human participating in the experiment. The body area was calculated from the formula given in [31]. The area for the mouth opening is equal to 1.3 cm^2 nad was based on data available in the literature [32–36]. This corresponds to dimensions $1.3 \text{ cm} \times 1.0 \text{ cm}$. Indoor air parameters were monitored in 15 points with first four monitors placed exact in the same places as the sensors in experiments.

3.2. Numerical grid

A hybrid grid was used to discretise the geometry of the model. In the central part of the considered room domain, structured grid was created. An unstructured grid was employed to discretise the remaining regions of the model. To be able to capture properly the flow fields near the breathing person surface and in the proximity of the small openings i.e. mouth, window and door gaps, the *Size Functions* were applied in those regions, see Fig. 5. *Size Functions* smoothly vary element sizes from very small near to openings to the size applied for the structured grid in the middle of the room. The grid element size varies form 0.1 m for structured grid in the middle of the room to 0.001 m for unstructured grid in the vicinity of the mouth, window and door cracks. The total number of the grid elements was equal to 684 825 for simplified geometry and 1 101 919 for an accurate model.

3.3. Numerical model

The air was modelled as an incompressible fluid consisting of four species, namely: oxygen (O₂), carbon dioxide (CO₂), water steam (H₂O) and nitrogen (N₂). Developed model consist of the following governing equations [37–40]:

3.3.1. Mass conservation equation (continuity equation)

$$\frac{\partial \varrho}{\partial t} + \nabla \cdot (\varrho \mathbf{u}) = 0 \quad (2)$$

where ϱ is density of fluid, t is time and \mathbf{u} refers to fluid velocity vector.

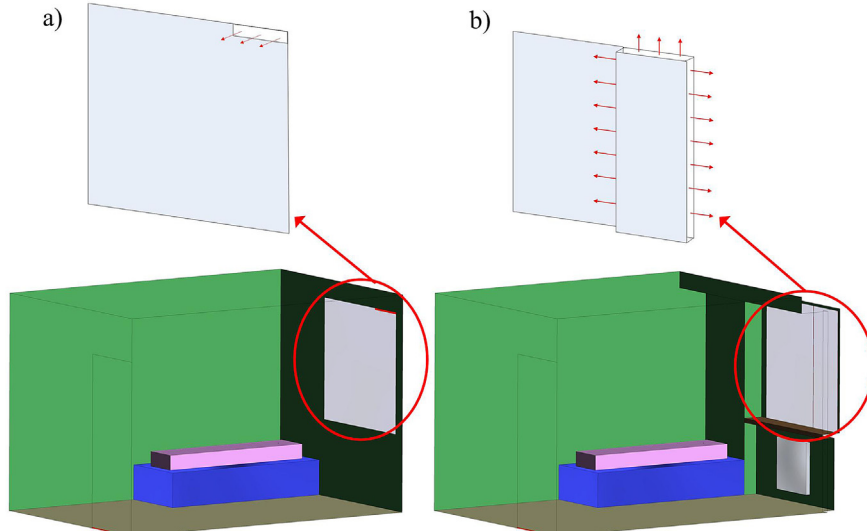


Fig. 4. Geometrical model of the room, a) simplified, b) accurate.

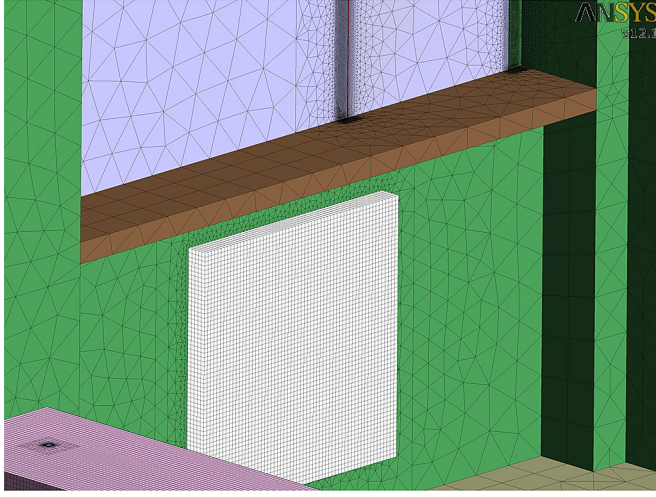


Fig. 5. Numerical grid of the room.

3.3.2. Conservation equations for air constituents

Partial differential transport equations of the three air constituents, namely O₂, CO₂ and H₂O where solved:

$$\frac{\partial(\varrho Y_{O_2})}{\partial t} + \nabla \cdot (\varrho Y_{O_2} \mathbf{u}) = -\nabla \cdot \mathbf{j}_{O_2} \quad (3)$$

$$\frac{\partial(\varrho Y_{CO_2})}{\partial t} + \nabla \cdot (\varrho Y_{CO_2} \mathbf{u}) = -\nabla \cdot \mathbf{j}_{CO_2} \quad (4)$$

$$\frac{\partial(\varrho Y_{H_2O})}{\partial t} + \nabla \cdot (\varrho Y_{H_2O} \mathbf{u}) = -\nabla \cdot \mathbf{j}_{H_2O} \quad (5)$$

The N₂ concentration was calculated from the sum of mass fractions of all air species which should be equal to unity:

$$Y_{N_2} = 1 - Y_{O_2} - Y_{CO_2} - Y_{H_2O} \quad (6)$$

where Y_i is mass fraction of i-th air constituent. Due to reasonably low thermal parameters (pressure and temperature) of air it can be treated as a rarified mixture. Hence, the mass flux of i-th constituent may be calculated using Fick's law:

$$\mathbf{j}_i = -D_{eff} \nabla Y_i \quad (7)$$

where D_{eff} is the effective diffusion coefficient which includes turbulence effects.

3.3.3. Momentum conservation equation

$$\frac{\partial(\varrho \mathbf{u})}{\partial t} + \nabla \cdot (\varrho \mathbf{u} \mathbf{u}) = -\nabla p + \varrho \mathbf{g} + \nabla \cdot (\mu \nabla \mathbf{u}) - \nabla \cdot \tau_t \quad (8)$$

where p is pressure, g is vector of gravitational acceleration, μ is molecular dynamic viscosity. The last term on the right hand side of the equation is divergence of the turbulence stresses (Reynolds stresses) τ_t , it accounts for auxiliary stresses due to velocity fluctuations. It is defined as follows:

$$\tau_t = \begin{bmatrix} \varrho \overline{u'^2} & \varrho \overline{u'v'} & \varrho \overline{u'w'} \\ \varrho \overline{u'v'} & \varrho \overline{v'^2} & \varrho \overline{v'w'} \\ \varrho \overline{u'w'} & \varrho \overline{v'w'} & \varrho \overline{w'^2} \end{bmatrix} \quad (9)$$

components of this tensor are average values of covariances of components of velocity vectors u', v' and w' appropriately in x, y and

z directions. Because fluctuations of velocity vector are unknown this term needs modelling [37,41].

3.3.4. Energy conservation equation

$$\frac{\partial(\varrho e)}{\partial t} + \nabla \cdot (\varrho e \mathbf{u}) = \nabla \cdot (k_{eff} \nabla T) - \nabla \cdot \left(\sum_i h_i \mathbf{j}_i \right) \quad (10)$$

where e is specific internal energy, k_{eff} is effective heat conductivity, T stands for fluid temperature, h_i refers to specific enthalpy of fluid.

3.3.5. Turbulence model equations

To close the system of governing equations terms related to turbulence effects, i.e. turbulent stresses, effective diffusivity and conductivity need to be modelled. In this work Boussinesq analogy was applied. According to this approach turbulent stresses are proportional to the gradient of the average velocity field:

$$\tau_{t,ij} = -\varrho \overline{u'_i u'_j} = \mu_t \left(\frac{\partial u_i}{\partial x_j} + \frac{\partial u_j}{\partial x_i} \right) - \frac{2}{3} \varrho \kappa \delta_{ij} \quad (11)$$

where μ_t is turbulent viscosity, κ is turbulent kinetic energy, a δ_{ij} refers to Kronecker delta. By analogy to Fourier and Fick laws it was assumed that turbulent heat and mass fluxes are proportional to gradients of average temperature and mass fraction appropriately [37,41]. The proportionality coefficients are turbulent heat conductivity k_t and turbulent diffusivity D_t . In differential conservation equations (3)–(5) and (10) this coefficients are summed up with their molecular counterparts giving effective quantities:

$$\begin{aligned} k_{eff} &= k + k_t \\ D_{eff} &= D + D_t \end{aligned} \quad (12)$$

where k is molecular heat conductivity and D stands for molecular diffusivity. In present work RNG (Renormalisation Group) $\kappa-\varepsilon$ turbulence model was used [42]. This model is very frequently used to simulate airflows dominated by natural convection [43–45]. In this model two additional transport equations for turbulent kinetic energy κ and dissipation rate of the turbulent kinetic energy ε :

$$\frac{\partial(\varrho \kappa)}{\partial t} + \nabla \cdot (\varrho \kappa \mathbf{u}) = \nabla \cdot [\alpha_\kappa \mu_{eff} \nabla \kappa] + G_\kappa + G_b - \varrho \varepsilon \quad (13)$$

$$\frac{\partial(\varrho \varepsilon)}{\partial t} + \nabla \cdot (\varrho \varepsilon \mathbf{u}) = \nabla \cdot [\alpha_\varepsilon \mu_{eff} \nabla \varepsilon] + C_{1\varepsilon} \frac{\varepsilon}{K} (G_\kappa + C_{3\varepsilon} G_b) - C_{2\varepsilon} \varrho \frac{\varepsilon^2}{K} \quad (14)$$

where G_κ stands for source of turbulent kinetic energy due to average velocity gradient, G_b is source of turbulent kinetic energy due to buoyancy force, α_κ and α_ε are turbulent Prandtl numbers, $C_{1\varepsilon}$, $C_{2\varepsilon}$ and $C_{3\varepsilon}$ are empirical model constants. Enhance Wall Treatment was applied for the flow near the wall.

The system of equations 2–14 were discretized using the Finite Volume Method and solved with use of the ANSYS Fluent commercial CFD (Computational Fluid Dynamic) software [40]. The unsteady calculations were made for the five hour period with a constant 0.1 s time step in case of a fully developed breathing model. In case of the simplified model with constant exhalation the time step was increased up to 10 s as the simulation proceeds.

The details of the numerical model, initial and boundary conditions applied in the model are listed in Tables 2 and 3. A pressure was prescribed at the door gap outflow and a mass flow rate was assumed at the window opening and at the person mouth. The air inlet velocity was assumed equal to 0.54 m/s. Moreover constant

Table 2
Numerical methods.

Equation	Numerical scheme
Continuity equation	PRESTO
Momentum equation	Second order upwind
Turbulence model equations (κ and ε equations)	Second order upwind
Energy equation	Second order upwind
Pressure–velocity coupling	SIMPLE

Table 3
Initial and boundary conditions.

Room air	$T = 19^\circ\text{C}$; $\phi = 39\%$; $\text{CO}_2 = 385 \text{ ppm}$
Room air inflow	$m = 0.00812 \text{ kg/s}$; $T = 10^\circ\text{C}$; $\phi = 60\%$; $C = 382 \text{ ppm}$
Room air outflow	Pressure outflow
Exhaled air	$T = 34^\circ\text{C}$; $\phi = 95\%$; $C = 36,000 \text{ ppm}$
Room wall	$T = 20^\circ\text{C}$ and $T = 19^\circ\text{C}$ for external wall
Human body	$T = 23.5^\circ\text{C}$ covered with duvet
Radiator	If on than $T = 60^\circ\text{C}$

Table 4
Mesh element size on the surface of the numerical model.

Surface	Coarse mesh	Fine mesh
Mouth, window, door gap	0.001 m	0.0005 m
Person, radiator	0.01 m	0.005 m
The rest of domain	0.1 m	0.05 m

value of temperature was assumed at the human body surface, at the internal walls surfaces and at the window surface.

In this work two models of the breathing were analysed: a constant exhalation and a full breathing cycle. In the literature few approaches to modelling of respiration process can be find [33,35,36,46–50]. A person performing a light physical work has an average respiration frequency equal to about 10 inhalation per minute. In each inhalation an approximate volume of 0.6 l of air is exchanged. The breathing cycle implemented in the model

consisted of inhalation period lasting 2.5 s, exhalation period lasting 2.5 s and 1 s pause period. Air exhaled by the person carrying out light work has temperature equal about 34°C and relative humidity equals about 95% [36]. For these data the instantaneous air flow rate during exhalation period equals to 14.4 l/min. The amount of the carbon dioxide in exhaled air was calculated from the formula given in [14,15] for the activity level of the sleeping person 0.7 met and is equal to 3.6% of the exhaled air. In the simplified model average value of 6 l/min of exhaled air was assumed.

4. Verification and validation of the numerical model

4.1. Mesh independent study

Mesh independent study was performed for two numerical grids. The coarse grid in the central domain of the numerical model had elements with size around 10 cm. The fine grid in the central region had element with size around 5 cm. Detailed information of the grid size in the vicinity of the human mouth, radiator and in the window and door gap are presented in Table 4. Further reduction of the mesh element size was restricted by computation time and computer resources. Increasing of the mesh element size to 20 cm would result in too coarse mesh giving unrealistic results.

It was found that results obtained with two different numerical grids differ not more than 45 ppm. The biggest discrepancies are found in the region just below the ceiling. In the lower part of the room carbon dioxide concentrations were almost the same. The difference of the average mass concentration in the fifth hour of calculation for both grids not exceeded 20 ppm. In Fig. 6 the numerically calculated carbon dioxide concentration obtained with both grids is compared with measured data in four monitoring places. It was observed that the numerically calculated carbon dioxide concentrations are slightly lower than the measured values.

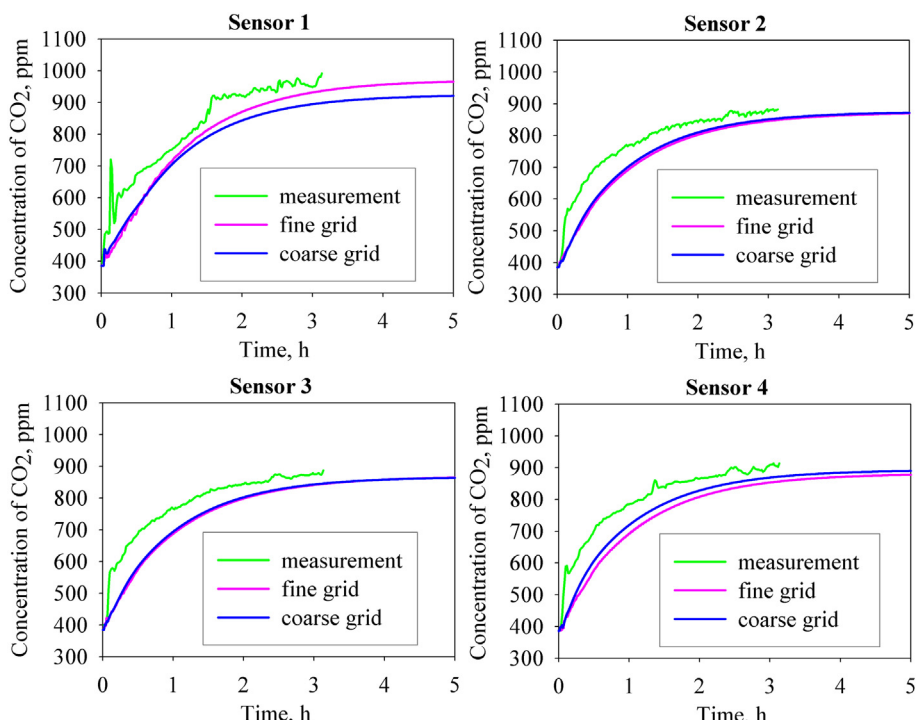


Fig. 6. Measured and calculated values of carbon dioxide concentration in four monitored places of the room.

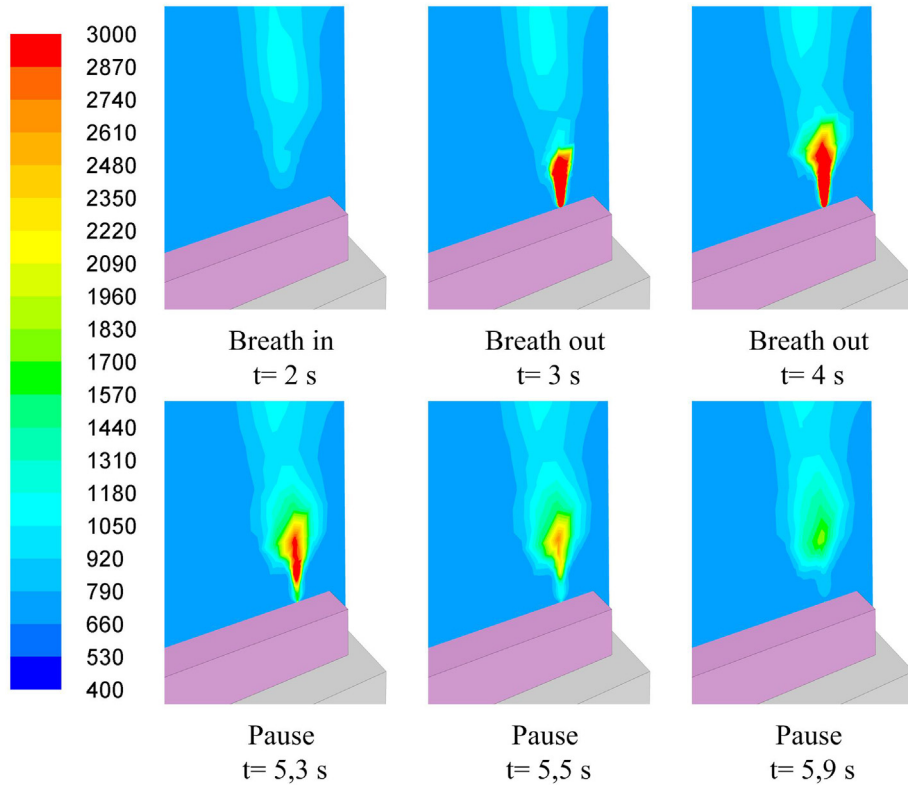


Fig. 7. Contours of carbon dioxide concentration (ppm) above the mouth for one breathing cycle.

After three hours calculations the differences between measured and calculated concentration was 16 ppm for the fine grid and 53 ppm for the coarse grid. Better agreement of the numerical and experimental results were find for the sensors 2 and 3. At the sensor point 1 placed under the ceiling the better results gives fine grid. At the sensor point 4 better result was obtained for coarse grid

with the difference of 40 ppm comparing to measurement and 55 ppm for fine grid. The difference of the measured and calculated carbon dioxide concentrations lay in the range of uncertainty of carbon dioxide monitor. Numerical calculation results obtained with the coarse grid were considered sufficiently precise. Therefore, all subsequent computations were done with use of the coarse

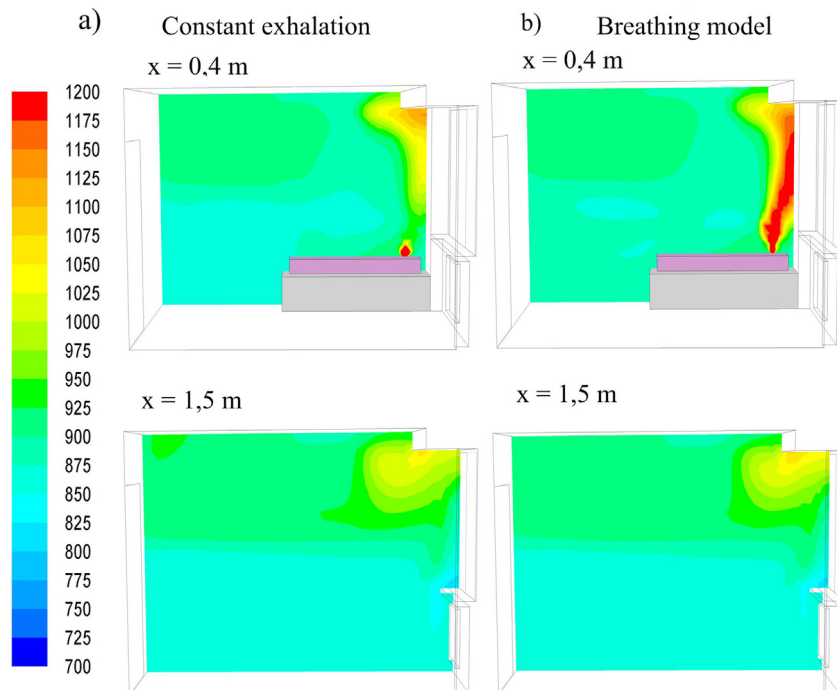


Fig. 8. Contours of carbon dioxide concentration (ppm) for a two breathing models on a vertical plane at $x = 0.4$ m and $x = 1.5$ m.

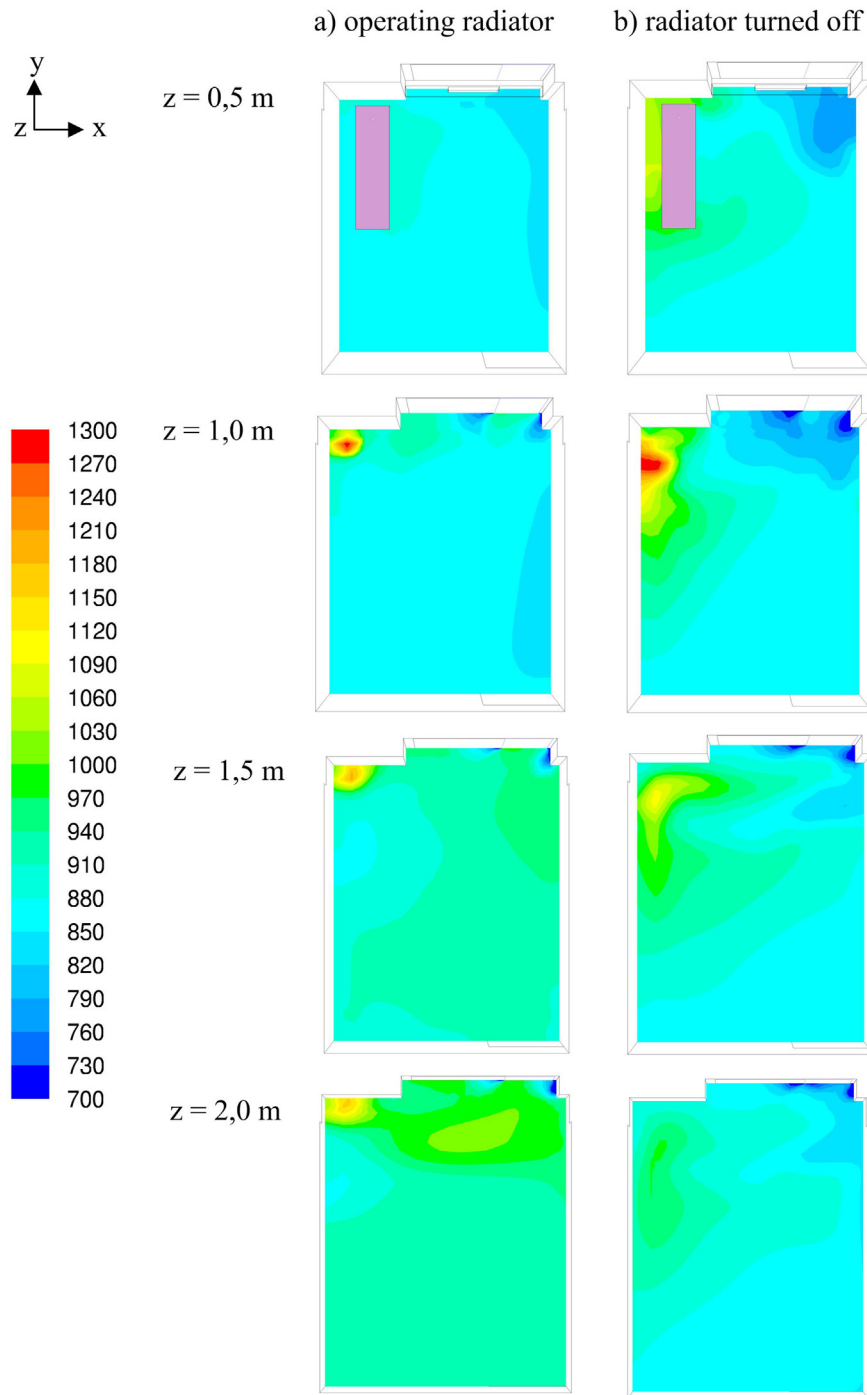


Fig. 9. Contours of carbon dioxide concentration for radiator turned off and radiator operating on a horizontal plane at $z = 0.5$ m, $z = 1.0$ m, $z = 1.5$ m and $z = 2.0$ m.

grid. The biggest advantage is receiving satisfactory results in reasonable time.

4.2. Verification of the crucial model parameters

4.2.1. Influence of the breathing model

Modelling of the breathing process can significantly influence the spatial distribution of the metabolic carbon dioxide within the room. Two breathing models were compared one simplified to constant exhalation and second with full birthing cycle (inhale,

exhale and pause). In Fig. 7 distribution of carbon dioxide concentration around the mouth in subsequent phase of the breathing cycle are presented. Model with full breathing cycle characterised with higher instantaneous velocity of exhaled air of 1.85 m/s in comparison to constant exhalation with a velocity of 0.77 m/s. This causes that the higher carbon dioxide concentration occurs in the upper part of the room. Small differences between carbon dioxide profiles calculated for both breathing models were observed only in the vicinity of the sleeping person. They disappear with the distance from the sleeping person

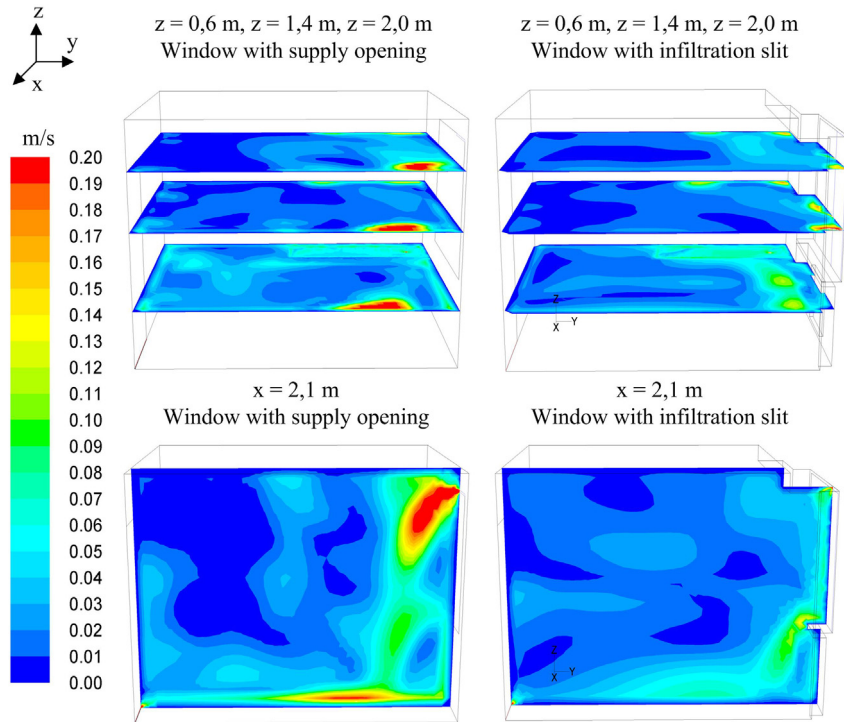


Fig. 10. Contours of airflow velocity for a window with supply opening and with infiltration slit on a horizontal plane at $z = 0.6$ m, $z = 1.4$ m, $z = 2.0$ m and on a vertical plane at $x = 2.1$ m.

(Fig. 8). Temporal changes of the carbon dioxide emission did not influence the spatial distribution of the carbon dioxide in the whole room [51].

4.2.2. Influence of the operating radiator

In the winter season air movements in the room is influenced by operating radiators. The air is heated up from the radiator surface and cool down by window surface. This cause the natural convection of the air in the room. It can also influence the spatial distribution of carbon dioxide. Two cases were analysed in the work one with radiator turned off and one with operating radiator at 60 °C. In Fig. 9 contours of carbon dioxide concentration for both cases are presented. In the room with radiator turned off higher stratification of carbon dioxide concentration was observed than in case with operating radiator. High concentration were observed under the ceiling and above the person. In case of the operating radiator air is much better mixed in the room. The high concentration of carbon dioxide were observe only directly above the sleeping person.

4.2.3. Influence of the inlet opening geometry

The next analysed factor that can influence the spatial distribution of the carbon dioxide in the room is the geometry of the air inlet. Two situations were compared. In the first case window was fitted with a supply opening at the top of the window. In the second analysed case the window was fitted with infiltration slit along the perimeter of the window leaf. The area of the opening in both cases was the same [51]. Simplification of the inlet opening geometry results in a different velocity profiles around the window and in the vicinity of the person as presented in Fig. 10. In case of window with infiltration slit the velocity of the air slow down very quickly. This results in slower air mixing in the room and higher stratification of carbon dioxide comparing to the case with supply opening in the window (see Fig. 11).

5. Determination of the representative regions of carbon dioxide concentration in the room

If only one sensor is used to record the CO₂ concentration than its position should be chosen carefully to be representative for average carbon dioxide concentration. Representative regions were determined based on the spatial distribution of carbon dioxide concentration computed using numerical simulations for two cases. In the first one the radiator was operating at the temperature 60 °C. In the second case the radiator was off. Both measurements and numerical computations are always carried out with finite precision. Hence, same tolerance level around average needs to be defined, while determining the representative regions. Three different tolerance levels were considered:

- **Tolerance level I**, $\pm 10\%$ average value of carbon dioxide concentration in the room. This tolerance interval is allowed by the standard [25,52] for carbon dioxide concentration oscillation within one zone,
- **Tolerance level II**, \pm accuracy of carbon dioxide sensors. Accuracy of the sensors in the measurements was equal to 20 ppm $\pm 3\%$ of measured value,
- **Tolerance level III**, ± 20 ppm, minimal estimated value of the measurements uncertainty.

Identification of the representative area within the room was carried out by analysing the horizontal sections of the whole room every 10 cm along the room height. It was done for every hour of the analysed process. It was found that the representative regions are getting smaller with time. Hence, results for the fifth hour of the process were used to obtain the final representative region for the room.

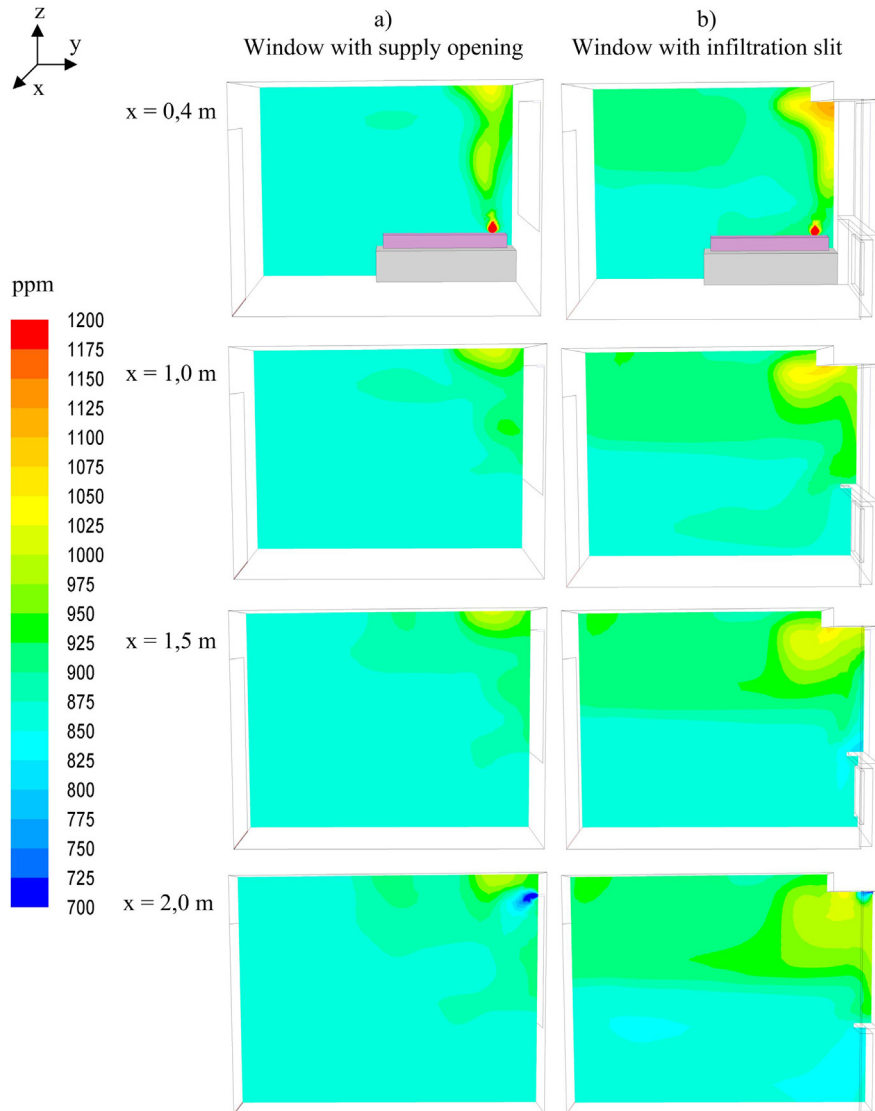


Fig. 11. Contours of carbon dioxide concentration for window with supply opening and with infiltration slit on a vertical plane at $x = 0.4\text{ m}$, $x = 1.0\text{ m}$, $x = 1.5\text{ m}$, $x = 2.0\text{ m}$.

5.1. Tolerance level I

In Fig. 12 representative regions of three particularly chosen horizontal sections, namely $z = 0.6\text{ m}$, $z = 1.2\text{ m}$, $z = 2.0\text{ m}$ are presented. In all of the presented section the representative region covers significant areas. The area with carbon dioxide concentration above the assumed tolerance appears in the vicinity of the bed and close to the window and radiator. In the case with the operating radiator this area is situated in the vicinity of the bed at the heights between 0.6 m and 1.5 m and if the radiator is off the same area appears in the vicinity of the bed and close to window at heights from 1.5 m to 2.2 m . Concentrations of the carbon dioxide below the assumed tolerance occurred only in the vicinity of the window gap. In case of this tolerance level the representative area does not change much with time, however it slightly decreasing with time.

The representative regimes identified on the horizontal room sections at different heights were utilised to find one common spatial representative regime of the analysed room. Its projection on the room floor is presented in Fig. 13. Common representative

regions covers over half of the room volume excluding the area around the bed (for the whole room height), the area around source of the carbon dioxide (with diameter of 1 m) and region around the window and radiator (with approximate distance of 1.5 m).

5.2. Tolerance level II

Representative regimes for the second tolerance interval are smaller than the tolerance level I. Concentrations below the tolerance developed along the wall adjacent to bed. Common representative region for the second tolerance level is presented in Fig. 13 and should be reduced by the area in the vicinity of the walls with the distance of at least 40 cm .

5.3. Tolerance level III

Tolerance of the carbon dioxide variations for tolerance level III is very strict. This cause that the representative region is very small. The area of higher carbon dioxide concentration appears in upper

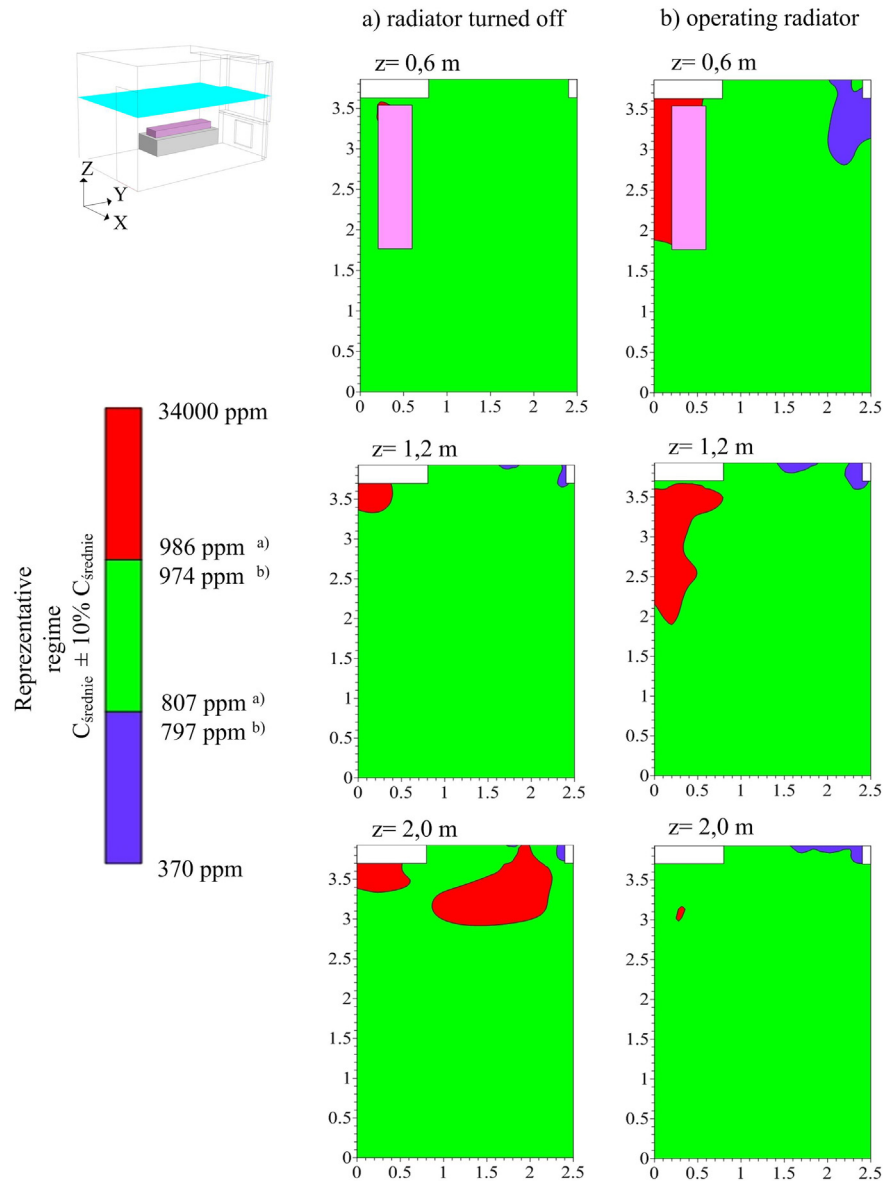


Fig. 12. Maps of carbon dioxide concentration (ppm) on the horizontal plane at different height for tolerance regime I, case a) with radiator turned off and b) with operating radiator.

part of the room for the case, with the radiator turned off and over the bed with sleeping person for the case with operating radiator. The area with concentration below assumed interval appears in the lower part of the room (below 1.2 m) in case with radiator turned off and in the vicinity of the window and the door for the case with operating radiator. The changes of carbon dioxide concentration with maximum 20 ppm for tolerance level III can be found only locally in the room. This caused that it was impossible to determinate a common region along the height of the room. The biggest representative region appeared at height from 1.4 to 1.5 m of the room for case with radiator turned off and at 2.2 m hight for operating radiator, it is shown in Fig. 14.

6. Results and discussion

Comparison of the measured and numerically computed carbon dioxide concentration showed small differences which are in the

range of the uncertainty of carbon dioxide sensors. It was found that the lowest concentrations appear in the lower part of the room and high concentrations can be observed near the ceiling. Results of verification of the numerical model allows one to formulate a conclusions:

- Spatial distribution of the carbon dioxide concentration in the room is only slightly affected by the breathing model applied in the simulation. Small differences in the concentration occurs only close to the person mouth. This can be important in case of modelling IAQ around human body only. For the modelling of the spatial distribution of carbon dioxide within the whole room the simplified breathing model is enough precise.
- The geometry of the modelling openings is very important for the distribution of the carbon dioxide in the room. In case of the window with micro-ventilation the air is slowly mixed

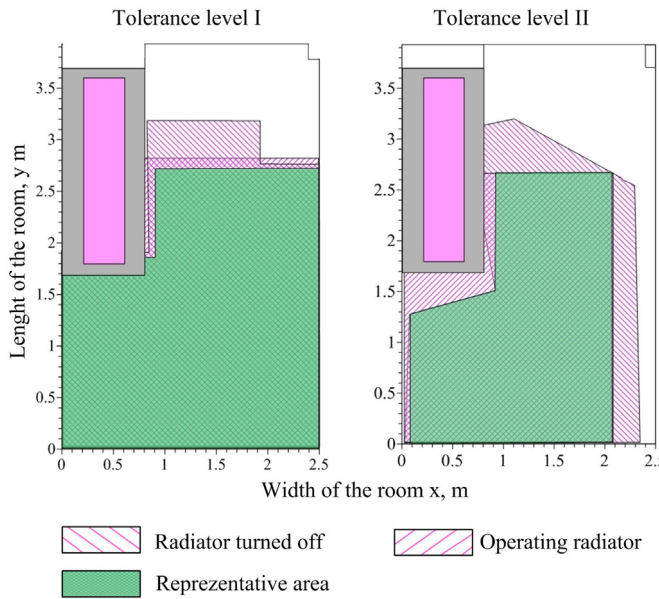


Fig. 13. Common representative area in tolerance levels I and II.

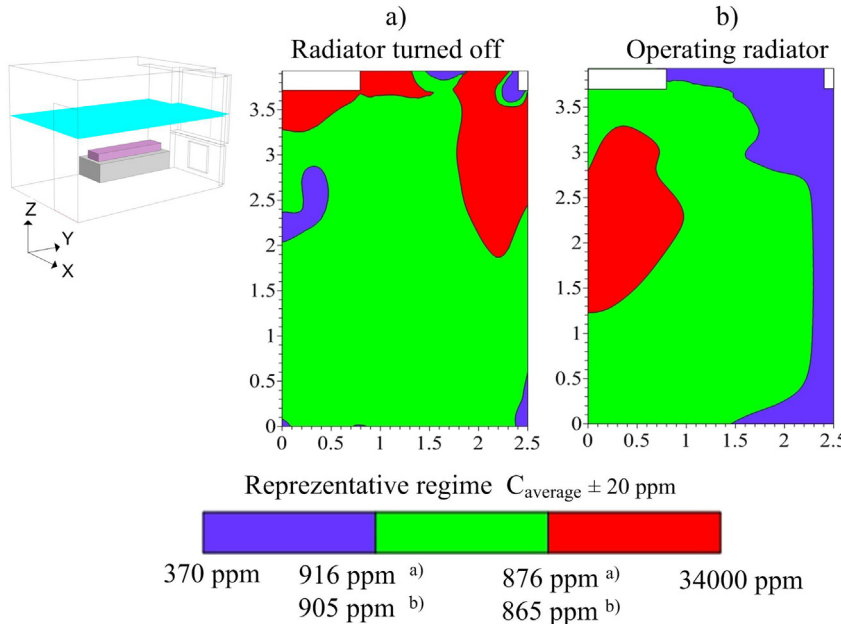


Fig. 14. Maximal representative regimes in tolerance level III for a case a) radiator turned off, height $z = 1.4 \text{ m}$ and b) operating radiator, height $z = 2.2 \text{ m}$.

in the room what cause the higher carbon dioxide stratification in the room. When the geometry of the window opening is simplified to a supply opening more homogenous concentration is obtained. Whereas too simple inlet opening gives unrealistic spatial distribution of the exhaled carbon dioxide.

- It is very important to take into a consideration a different conditions which appears in the room for a different weather seasons of the year. Radiator operating in the room generates convection plume which influence the spatial distribution of CO_2 in the room. This causes the necessity to include all heat sources into the mathematical model of the airflow.

The main goal of the work was determination of the representative regions of carbon dioxide concentration

measurement in the room. Three tolerance levels were confederated. It was found that the common representative regions were situated in the centner of the room, however for the very rigorous tolerance level III this area can be identified only in the middle of the room hight while for two others tolerance levels it can be identified along the whole hight of the room. What is more, received results allows one to express the general statements useful in positioning of the carbon dioxide sensor in the room:

- The measurements should not be taken above the source of carbon dioxide emission. In case of the breathing person whole volume above the bed should be excluded from the measurements.
- Measurements should be taken in same distance from the heat sources like radiators and inlet openings in the window.
- The distance of the sensors from the wall should be at least 40 cm.
- The most favourable regions for carbon dioxide concentration is the centre of the room.

7. Conclusions

This study showed that the numerical simulations can be successfully used to predict spatial distribution of carbon dioxide exhaled by person in a room. Results of numerical calculations lay in the tolerance of the experimental data. Results showed how strongly the spatial distribution of carbon dioxide is influenced by the geometry of the window opening and operating radiator. It was also found that the simplified model of breathing person is enough precise for such a calculations. Results presented in the work shows that carbon dioxide concentration in the room with breathing person is not homogenous. However it is possible to find a representative regions in which carbon dioxide concentration is in assumed range around the average concentration of the whole room. Results presented in the work showed the places

which should be avoided during the measurements like the region around the breathing person in the vicinity of window and radiator. It was found that the representative measurements of carbon dioxide concentration can be successfully done in the centre of the room.

The study was carried out for a typical bedroom in a multifamily flat. Results of this study can not be generalised for all the type of the rooms. Analysis of the spatial distribution of carbon dioxide in a room with different geometry and room furniture should also be preformed. Moreover influence of the different air exchange rate should also be checked. This is considered for future work.

References

- [1] Dimitroulopoulou C. Ventilation in European dwellings: a review. *Build Environ* 2012;47:109–25.
- [2] Nantka MB. Indoor climate and energy consumption in buildings with natural ventilation. ACEE – Archit, Civil Eng, Environ 2008;1(3):107–18.
- [3] Santamouris M, Synnefa A, Assimakopoulos M, Livada I, Pavlou K, Papaglastra M, et al. Experimental investigation of the air flow and indoor carbon dioxide concentration in classrooms with intermittent natural ventilation. *Energy Build* 2008;40:1833–43.
- [4] Griffiths M. Control of CO₂ in naturally ventilated classroom. *Energy Build* 2008;40:556–60.
- [5] Beko G, Nors F, Toftum J, Clausen G. Carbon dioxide concentrations and ventilation rates in 500 danish homes: indoor environment and children's health (iech) study. In: 9th International conference and exhibition, healthy buildings, Syracuse, USA 2009, paper 383.
- [6] McWilliams J. Review of air flow measurement techniquesIn Paper posted at the eScholarship Repository. Lawrence Berkeley National Laboratory, University of California; 2002. <http://repositories.cdlib.org/lbl/LBNL-49747>.
- [7] Allard F. Natural ventilation in buildings. London, United Kingdom: James & James Science Publishers; 1998.
- [8] Barankova P, Naydenov K, Melikov A, Sundell J. Distribution of carbon dioxide produced by people in a room: Part 1-laboratory study. In: Proceedings of Roomvent. Portugal: University of Coimbra; 2004.
- [9] Barankova P, Sundell J, Melikov A, Naydenov K. Distribution of carbon dioxide produced by people in a room: Part 2- field study. In: Proceedings of Roomvent. Portugal: University of Coimbra; 2004.
- [10] Mahyuddin N, Awbi H. The spatial distribution of carbon dioxide in an environmental test chamber. *Build Environ* 2010;45:1993–2001.
- [11] Mahyuddin N, Awbi H. A review of CO₂ measurement procedures in ventilation research. *Build Environ* 2012;10(4):353–70.
- [12] Gadyszewska-Fiedoruk K. Analysis of stack ventilation system effectiveness in an average kindergarten in north-eastern poland. *Energy Build* 2011;43: 2488–93.
- [13] Nantka MB. Airtightness and natural ventilation: a case study for dwellings in Poland. *J Vent* 2005;4(1):79–91.
- [14] ASTM standard D 6245-07 standard guide for using indoor carbon dioxide concentration to evaluate indoor air quality and ventilation. American Society for Testing and Materials; 2002.
- [15] Persily AK. Evaluating building IAQ and ventilation with indoor carbon dioxide. *ASHRAE Transaction* 1997;103(2):193–204.
- [16] Liddament M. Why CO₂? *Air Infiltration Review* 1996;18(1):1–7.
- [17] CEN CR 1752. Ventilation for buildings – design criteria for the indoor environment. European Committee for Standardization; 1998.
- [18] ASHRAE 62-1989. Ventilation for acceptable indoor air quality. American Society of Heating, Refrigerating and Air-Conditioning Engineers; 1989.
- [19] Clements-Croome DJ. Ventilation rates in schools. *Build Environ* 2008;43: 362–7.
- [20] Aglan Heshmat A. Predictive model for CO₂ generation and decay in building envelopes. *J Appl Phys* 2003;93(2):1287–90.
- [21] Penman JM. An experimental determination of ventilation rate in occupied rooms using atmospheric carbon dioxide. *Build Environ* 1980;15:45–7.
- [22] Penman JM, Rashid AAM. Experimental determination of air-flow in a naturally ventilated room using metabolic carbon dioxide. *Build Environ* 1982;17(4):253–6.
- [23] Smith PN. Determination of ventilation in occupied buildings from metabolic carbon dioxide concentration and production rates. *Build Environ* 1988;23(2): 253–6.
- [24] Mui KW, Wong LT, Ho WL. Evaluation on sampling point densities for assessing indoor air quality. *Build Environ* 2006;41:1515–21.
- [25] ASTM E 741–00. Standard test method for determining air change in a single zone by means of a tracer gas dilution. American Society for Testing and Materials; 2000.
- [26] Son CH. Computational fluid dynamics simulation helps protect astronauts in space station from CO₂. *Journal Articles by F L U E N T Software Users*.
- [27] Mahyuddin N, Awbi H. Modelling the distribution of the exhaled CO₂ in an environmental chamber. In: 10th International conference, healthy buildings 2012 2012.
- [28] Braun JE, Lawrence TM. Evaluation of the simplified models for predicting CO₂ concentrations in small commercial buildings. *Build Environ* 2006;41:184–94.
- [29] Bulińska A. Determination of airflow pattern in a residential building using metabolic carbon dioxide concentration measurements. page 188. In: 10th International conference on air distribution in rooms. SCANVAC conference, Roomvent 2007, Helsinki, Finland 2007.
- [30] Deevy M, Gobeau N. CFD modelling of benchmark test cases for a flow around a computer simulated person. HSL/2006/51. Buxton,UK: Health and Safety Laboratory; 2006.
- [31] ASHRAE fundamentals handbook. Atlanta: American Society of Heating, Refrigerating and Air-Conditioning Engineers; 2001.
- [32] Brohus H. Personal exposure to contaminant sources in ventilated rooms [PhD thesis]. Denmark: Aalborg University; 1997.
- [33] Hayashi T, Ishizu Y, Kato S, Murakami S. CFD analysis on characteristics of contaminated indoor air ventilation and its application in the evaluation of the effects of contaminant inhalation by a human occupant. *Build Environ* 2002;37:219–30.
- [34] Iving M, Garrard A, Gobeau N, Mark D. Feasibility study of modelling particle deposition onto a person using computational fluid dynamics. HSL/2006/82. Buxton,UK: Health and Safety Laboratory; 2006.
- [35] Gao N, Niu J. Transient CFD simulation of the respiration process and inter-person exposure assessment. *Build Environ* 2006;41:1214–22.
- [36] Hyldgaard EC. Humans as a source of heat and air pollution. In: Forth International conference on air distribution in rooms Roomvent 1994, Cracow, Poland 1994.
- [37] Versteeg HK, Malalasekera W. Computational fluid dynamics. The finite volume method. Loughborough: Longman Scientific and Technical; 1995.
- [38] Ferziger JH, Peri M. Computational methods for fluid dynamics. Springer; 2002.
- [39] White FM. Fluid mechanics. McGraw-Hill; 2008.
- [40] Ansys. Fluent product documentation.
- [41] Pope SB. Turbulent flows. Cambridge University Press; 2009.
- [42] Yakhot V, Orszag SA. Renormalisation group analysis of turbulence i. basic theory. *J Sci Comput* 1986;1:3–51.
- [43] Zhang Z, Zhang W. Evaluation of various turbulence models in predicting airflows and turbulence in enclosed environments by CFD: Part 2-comparison with experimental data from literature. *HVAC Res* 2007;13(6):871–86.
- [44] Awbi HB. Ventilation of buildings. London: Taylor and Francis Group; 2003.
- [45] Nielsen PV, Allard F, Awbi HB, Davidson L, Schlin A. Computational fluids dynamics in ventilation design. Rehva guidebook 10, 2007.
- [46] Melikov A, Kaczmarczyk J. Measurement and prediction of indoor air quality using a breathing thermal manekin. *Indoor Air* 2007;17:50–89.
- [47] Ameziane I, Awada A, Sawan M. Modelling and simulation of an infant's whole body plethysmograph. *Build Environ* 2004;39:795–805.
- [48] Gao N, Niu J. Cfd study on micro-environment around human body and personalized ventilation. *Build Environ* 2004;39:795–805.
- [49] Gao N, Niu J. Cfd study of thermal environment around a human body: a review. *Indoor Build Environ* 2005;14(1):5–16.
- [50] Murakami S. Analyses and design of micro-climate around the human body with respiration by CFD. *Indoor Air* 2004;14(7):114–56.
- [51] Bulińska A. Computational and experimental investigation of the metabolic carbon dioxide propagation within a room. page 241. In: 10th Rehva World Congress. Clima 2010, Antalya, Turkey 2010.
- [52] EN ISO 12569:2012: Thermal performance of buildings and materials – determination of specific airflow rate in buildings – tracer gas dilution method, ISO Standard, 2012.